Near-infrared cathodoluminescence imaging of defect distributions in $In_{0.2}Ga_{0.8}As/GaAs$ multiple quantum wells grown on prepatterned GaAs

D. H. Rich, K. C. Rajkumar, Li Chen,[a] and A. Madhukar[a]
Photonic Materials and Devices Laboratory, Department of Materials Science and Engineering, University of Southern California, Los Angeles, California 90089-0241

F. J. Grunthaner
Center for Space Microelectronics Technology, Jet Propulsion Laboratory, California Institute of Technology, Pasadena, California 91109

(Received 18 October 1991; accepted for publication 25 April 1992)

The defect distribution in a highly strained $In_{0.2}Ga_{0.8}As/GaAs$ multiple-quantum-well (MQW) structure grown on a patterned GaAs substrate is examined with cathodoluminescence imaging and spectroscopy in the near infrared. By spatially correlating the luminescence arising from the MQW exciton recombination ($\lambda \approx 950$ nm) with the longer wavelength ($1000 \lesssim \lambda \lesssim 1200$ nm) luminescence arising from the defect-induced recombination, we demonstrate that it is possible to determine the regions of highest film quality in both the mesa and valley regions. The present approach enables a judicious determination of the optimal regions to be used for active pixels in InGaAs/GaAs spatial light modulators.

Presently, there is a considerable level of interest in using selective-area epitaxial growth approaches to achieve the fabrication of thick pseudomorphic films of strained $In_xGa_{1-x}As$ and related multiple-quantum-well (MQW) structures on GaAs substrates. Previous studies employing transmission electron microscopy (TEM),[1-4] photoluminescence (PL),[2,5] cathodoluminescence (CL),[6] optical absorption,[1,3] and micro-Raman[4] have demonstrated a substantial reduction in the density of misfit dislocations occurring in thick $In_xGa_{1-x}As$ films and MQWs grown on GaAs mesas with dimensions between 1 and 400 μm. In order to optimize the procedure by which to fabricate functioning device arrays having such lateral dimensions, it is essential to be able to elucidate the optical and structural properties on the scale of a micrometer or less.

In this letter, we employ the technique of cathodoluminescence scanning electron microscopy (SEM) to examine spatial and spectral variations in the defect-induced near-infrared luminescence of a thick MQW structure of $In_{0.2}Ga_{0.8}As/GaAs$ grown by molecular-beam epitaxy (MBE) on a prepatterned GaAs substrate. The present study demonstrates the complex interplay between the mesa side walls and the growth kinetics in the valley regions. These results are expected to influence current thinking regarding the design and fabrication of spatial light modulator device arrays requiring the highest possible material quality in isolated pixel regions.[3,7]

The n^+-type GaAs(100) substrate was patterned using conventional optical lithography and wet chemical etching.[1-3] The crystallographically selective etch results in undercut and inclined sidewall planes at the mesa edges. The resulting mesas had dimensions of about 2 μm $\times$ 16 μm $\times$ 18 μm with a 40-μm pitch in both directions before MBE growth. A SEM image of a typical mesa is shown in Fig. 1. The structure consists of a 100-period $In_{0.2}Ga_{0.8}As$ (80 Å)/GaAs (160 Å) MQW (having $\sim$2.38 μm total thickness) with a 5000-Å p^+-type GaAs capping layer. Cross-sectional TEM and absorption results of this sample (designated RG891110) have been previously described.[1,3] Cathodoluminescence measurements were performed at the Jet Propulsion Laboratory.[8] An electron beam current of 0.5 nA at an accelerating voltage of 40 kV was used to probe the sample for the CL measurements. The sample was maintained at a temperature of $\sim$77 K.

A SEM image of the structure showing a 220 μm $\times$ 170 μm area is presented in Fig. 2(a). Scanning monochromatic CL images corresponding to the same region are shown in Figs. 2(b)–2(d) for wavelengths of 950, 1040, and 1120 nm, respectively. Regions of increasing luminescence signal are represented by areas of lighter shades. The image with $\lambda = 950$ nm [in Fig. 2(b)] shows a hatched region of bright luminescence with maximum intensity in the valley regions midway along the [010] diagonal (dotted line in Fig. 1) between mesa centers. There is some observable emission from the centers and edges of the mesas at this wavelength. A dark halo region is found to surround the mesas, where little emission is detected. As the wavelength is increased to 1040 and 1120 nm, the images in Fig. 2 show an enhanced emission from the centers and sides of the mesas relative to the valley regions. Also, for these wavelengths the luminescence patterns on top of most of the mesas show a distinct dumbbell shape with maximal intensity near the mesa edges parallel to [1$\bar{1}$0], as seen in Figs. 2(c) and 2(d).

In order to further quantify the spatial distribution of the luminescence, we have performed a set of line scans over the single mesa which is depicted in the SEM image of Fig. 1. In Fig. 3, the CL intensity for the three different wavelengths of 840, 950, and 1120 nm are plotted as a function of the electron-beam position (ΔX) along the dashed and solid lines in Fig. 1 which are oriented along [110] and [1$\bar{1}$0], respectively. The arrows in Fig. 1 indicate an increasing ΔX in the line scan which has its origin at the intersection of the dashed and solid lines; the point labeled

[a]Also with Department of Physics, University of Southern California.

 0003-6951/92/270222-03$03.00 © 1992 American Institute of Physics

Downloaded 21 Jun 2007 to 132.72.138.1. Redistribution subject to AIP license or copyright, see http://apl.aip.org/apl/copyright.jsp

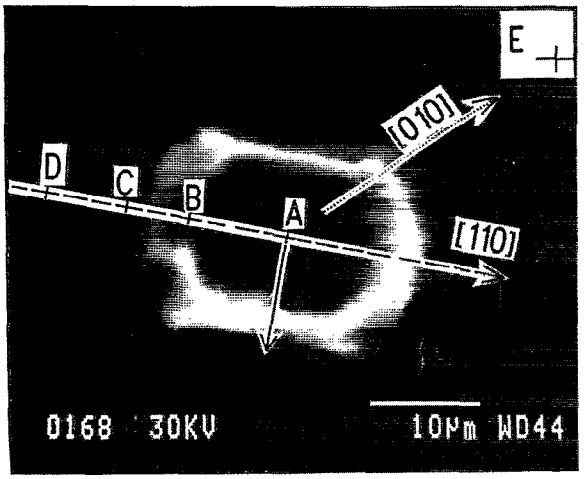

FIG. 1. SEM micrograph of a typical mesa of the $In_{0.2}Ga_{0.8}As/GaAs$ MQW structure. The dashed and solid lines with arrows oriented along [110] and [1$\bar{1}$0], respectively, indicate the position of the electron beam during line scans. Points A–E indicate beam position during local CL spectroscopy.

A ($\Delta X=0$) is located in the approximate center of the mesa.

These results were further investigated by localized CL spectroscopy of the region depicted in the SEM image of Fig. 1. The electron beam was fixed at certain points indicated in Fig. 1 with tic marks (labeled A, B, C, D, and E), and CL spectra, as presented in Fig. 4, were taken. Multiplication factors used to scale the absolute intensity of the spectra are indicated. The peak at $\lambda=840$ nm is the result of emission from the GaAs capping layer. The sharp Gaussian-shaped peak at $\sim$950 nm is the MQW e-hh exciton transition which has a large variation in intensity dependent on the beam position. From the two line scans of Fig. 3, the $\lambda=950$ nm peak is seen to maximize at positions of $\Delta X\approx\pm 20$ μm from the center of the mesa. Further inspection of the CL image of Fig. 2(b) and the local spectra in Fig. 4 at point E ($\sim$28 μm from point A), however, indicates that the regions halfway along the [010] diagonal between mesa centers yield the strongest exciton peak intensity. A strong emission in the $1000\lesssim\lambda\lesssim 1200$ nm region (in Fig. 4) is observed for certain points A and B on the mesa; two broad bands centered at $\lambda\approx 1040$ nm and $\lambda\approx 1100$ nm are seen. Previously, from photoluminescence of single $In_{0.17}Ga_{0.83}As$ QWs having various thicknesses, a long wavelength luminescence was found in the $1000\lesssim\lambda\lesssim 1600$ nm region.[9] This was attributed to presence of interface defects, such as misfit dislocations at the InGaAs/GaAs interface. Thus, it is reasonable to attribute the longer wavelength CL emission to the presence of structural defects which have previously been observed in cross-sectional TEM of this sample.[1,3] The difference in these two types of structures (single QW vs MQW and In alloy composition) would naturally give rise to differences in defect types and densities, and would therefore yield different luminescence spectra. The defect-induced luminescence is seen to be strongest near $\Delta X\approx\pm 6$ μm in the $\lambda=1120$ nm line scan of Fig. 3, which is near the centers of dumbbell-shaped lobes seen in the CL images. The exciton emission is markedly reduced at point B ($\Delta X=-9$ μm)

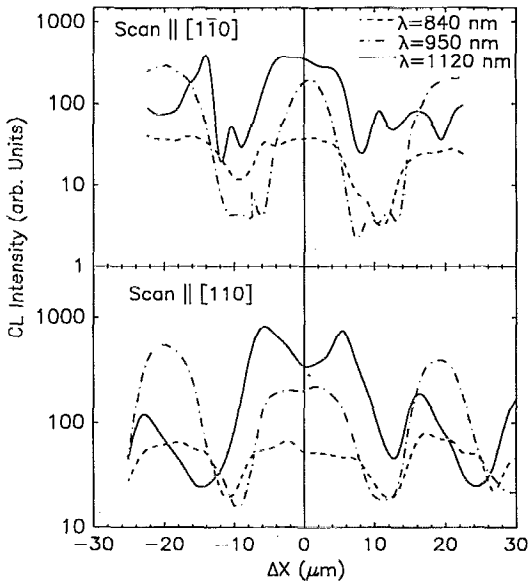

FIG. 3. Cathodoluminescence monochromatic line scans along the solid and dashed lines depicted in Fig. 1; $\Delta X=0$ corresponds to point A in Fig. 1.

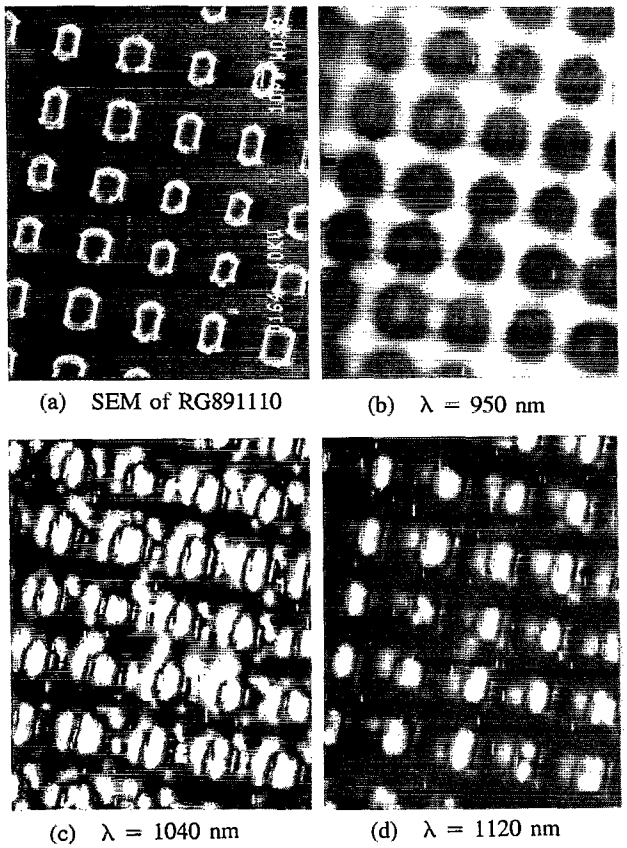

FIG. 2. SEM (a) and scanning monochromatic cathodoluminescence images [(b), (c), and (d) correspond to wavelengths of 950, 1040, and 1120 nm, respectively] of the same region of the $In_{0.2}Ga_{0.8}As/GaAs$ MQW structure.

Downloaded 21 Jun 2007 to 132.72.138.1. Redistribution subject to AIP license or copyright, see http://apl.aip.org/apl/copyright.jsp

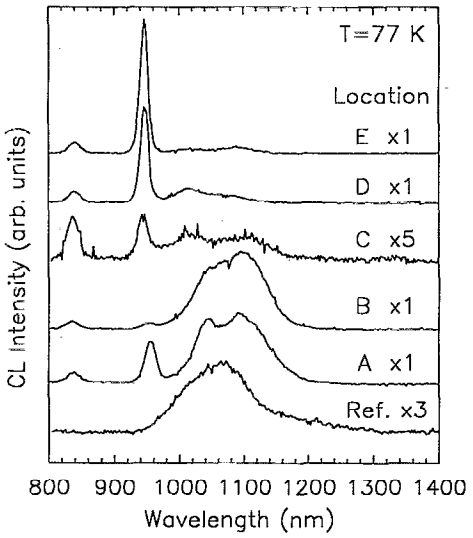

FIG. 4. Localized cathodoluminescence spectroscopy at the points A–E shown in Fig. 1. The sample labeled *Ref* corresponds to the spectrum taken in the nonpatterned region of the $In_{0.2}Ga_{0.8}As/GaAs$ MQW structure.

which is near the edge of the mesa in Fig. 1. This is consistent with enhancement of the defect-induced emission at point B since a large presence of defect-related recombination channels are expected to compete with the exciton recombination and reduce the total carrier lifetime.

The electron beam was further positioned within the dark halo region surrounding the mesa [see Fig. 2(b)] at point C ($\Delta X = -15$ μm) in Fig. 1. A significant decrease in both the exciton- and defect-related features is seen. Thus, the presence of additional *nonradiative* recombination channels caused by changes in the defect distribution dominate the carrier lifetime in this region. The electron-beam positions D ($\Delta X = -22$ μm) and E yield CL spectra with a large increase in the exciton luminescence and simultaneous reduction in the defect feature. Also at point E, the largest exciton-to-defect emission ratio was found; this indicates the region with the best-film quality. The spectrum labeled *Ref* in Fig. 4 corresponds to a point on the nonpatterned region of the sample. Only a broad and shifted defect-related band is observed with no exciton emission. This is consistent with the marked reduction in the threading dislocation density in the patterned region relative to the nonpatterned region, as previously observed in cross-sectional TEM.[1,3]

The dumbbell shape on the mesas, as seen in the $\lambda \geqslant 1000$ nm CL images and the [110] CL line scan, indicates the presence of interfacet cation migration in which the In migrates up along the inclined edges. The presence of contiguous low index planes is known to cause interfacet migration; this behavior has been observed to cause compositional variations in the AlGaAs and InGaAs films grown on patterned substrates.[1–3,5,10] The wavelength positions of the exciton peak at points A and E are 954 and 946 nm, respectively. If attributed exclusively to a variation in the In content, this shift corresponds to an In compositional change upper limit of $\sim 0.5\%$.[11] This is too small a shift to alone account for the extreme defect-induced luminescence variations observed here. The specific structural nature of the defects responsible for the long-wavelength luminescence cannot be determined from the present study. The defect-induced emission is, however, likely influenced by the proximity of the region to the growth on the contiguous (111) and higher index facets and the attendant interfacet cation migration. It is often desirable to eliminate the effects of cation migration on the faceted walls altogether by growing on elongated [110] striped mesas.[2,5]

In conclusion, we have demonstrated the effectiveness of cathodoluminescence imaging and spectroscopy in the near infrared in determining the spatial distribution of the defect-induced bands and exciton line for an InGaAs MQW grown on patterned GaAs. The presence of inclined mesa edges and cation migration is seen to influence the defect distribution for this particular class of patterned MBE growth. The presence of a characteristic dumbbell shape in the defect-induced luminescence pattern suggests that these regions are far from ideal for applications in spatial light modulators. Instead, regions midway between the mesa centers yield extremely large exciton-to-defect luminescence ratios. This suggests that these regions, with further device processing, could serve as *high-contrast-ratio* light modulators.[3,7]

At the University of Southern California, part of this work was supported by the Air Force Office of Scientific Research, University Research Initiative, Defense Advanced Research Projects Agency (DARPA), and Office of Naval Research. Other parts were performed by the Center for Space Microelectronics Technology, Jet Propulsion Laboratory, Caltech, and were jointly sponsored by DARPA and National Aeronautics and Space Administration, Office of Aeronautics, Exploration, and Technology.

[1] A. Madhukar, K. C. Rajkumar, L. Chen, S. Guha, K. Kaviani, and R. Kapre, Appl. Phys. Lett. **57**, 2007 (1990).
[2] S. Guha, A. Madhukar, and L. Chen, Appl. Phys. Lett. **56**, 2304 (1990).
[3] L. Chen, K. Hu, K. C. Rajkumar, S. Guha, R. Kapre, and A. Madhukar, *Proceedings of the MRS Symposium on Materials for Optical Information Processing*, Anaheim, CA, Vol. 240, May 1–3, 1991 (in press).
[4] W. C. Tang, H. J. Rosen, S. Guha, and A. Madhukar, Appl. Phys. Lett. **58**, 1644 (1991).
[5] Y. Zou, P. Grodzinski, J. S. Osinski, and P. D. Dapkus, Appl. Phys. Lett. **58**, 717 (1991).
[6] E. A. Fitzgerald, G. P. Watson, R. E. Proano, and D. G. Ast, P. D. Kirchner, G. D. Pettit, and J. M. Woodall, J. Appl. Phys. **65**, 2220 (1989).
[7] K. Hu, L. Chen, A. Madhukar, P. Chen, K. C. Rajkumar, K. Kaviani, Z. Karim, C. Kyriakakis, and A. R. Tanguay, Jr., Appl. Phys. Lett. **59**, 1108 (1991), and references therein.
[8] D. H. Rich, A. Ksendzov, R. W. Terhune, F. J. Grunthaner, B. A. Wilson, H. Shen, M. Dutta, S. M. Vernon, and T. M. Dixon, Phys. Rev. B **43**, 6836 (1991).
[9] M. J. Joyce, M. Gal, and J. Tann, J. Appl. Phys. **65**, 1377 (1989).
[10] For migration in AlGaAs, see, e.g., S. Guha, A. Madhukar, K. Kaviani, L. Chen, R. Kuchibhotla, R. Kapre, M. Hyugaji, and Z. Xie, Mater. Res. Soc. Proc. **145**, 27 (1989).
[11] K. F. Huang, K. Tai, S. N. G. Chu, and A. Y. Cho, Appl. Phys. Lett. **54**, 2026 (1989).

Downloaded 21 Jun 2007 to 132.72.138.1. Redistribution subject to AIP license or copyright, see http://apl.aip.org/apl/copyright.jsp